A methodology for including the effect of dissipative treatments in the mid-frequency domain using SmEdA method - Comparison with experiments

Ha Dong Hwang, Kerem Ege, Laurent Maxit, Nicolas Totaro, Jean-Louis Guyader

A methodology for including the effect of dissipative treatments in the mid-frequency domain using SmEdA method – Comparison with experiments.

Ha Dong Hwang, Kerem Ege, Laurent Maxit, Nicolas Totaro and Jean-Louis Guyader

Univ Lyon, INSA-Lyon, Laboratoire Vibrations Acoustique,
F-69621 Villeurbanne, France

Statistical modal Energy distribution Analysis (SmEdA) can be used to model a fluid-structure problem based on modal information of the uncoupled-subsystems. Recently, the method has been extended to include the effect of a dissipative treatment (i.e. damping or absorbing material). In this paper, SmEdA is tested on a steel plate with/without damping treatment coupled to an acoustic cavity: the numerical result of the energy ratio is compared to experimental one. The data are analyzed for a mid-to-high frequency domain (up to 10 kHz in 1/3 octave band). Both subsystem loss factors are experimentally obtained by a high-resolution modal analysis method based on the ESPRIT algorithm applied to impulse responses of the plate and the cavity. Predicting the energy level requires an accurate estimation of subsystem damping levels. The uncertainty on measured loss factors leads to an uncertainty in the energy ratio depending on min/max damping levels of individual modes in a given frequency band. Once min/max damping levels of subsystems are determined, SmEdA is used to compute the upper and lower limits of the subsystem energy ratio. A comparison with experimental results shows that the measurement data fits in between the SmEdA bounds. In this paper, two types of dissipative treatments are studied: i) a viscoelastic patch on the plate (modeled as an equivalent single layer plate) and ii) a porous material inside the cavity (modeled as an equivalent fluid).

1 Introduction

Statistical modal Energy distribution Analysis (SmEdA) [1] is an effective method to study many coupled problems in a mid-high frequency domain. The method has been recently extended to investigate the influence of an additive damping material applied to a structural subsystem in a plate-cavity coupled problem. The part of the plate treated with a viscoelastic damping pad was modeled as an equivalent property of the plate subsystem [2].

In this paper, the focus is on the analogous concept of the equivalent property modeling of an additive damping applied to a cavity subsystem. When a porous material is placed inside an air-filled cavity, it can be integrated into a cavity subsystem as an equivalent fluid. Such modeling greatly reduces the size of the finite element subsystem to be solved thus leads to more efficient SmEdA implementation. At the end, the aim of the study is to investigate the influence of different dissipative materials over subsystem energy flow. Numerically obtained subsystem energy levels and their ratio will be discussed and compared to experimental results.

Since the energy exchange between subsystems is affected by subsystem damping levels, it is important to obtain accurate data. The subsystem damping loss factors are experimentally estimated with the high-resolution modal analysis method based on the ESPRIT algorithm [3] from the impulse response of each subsystem. The loss factors are deduced from a number of selected resonant modes in 1/3 octave bands. As damping levels of individual modes can significantly vary within each frequency band, this variation can be used to set limits for a subsystem energy ratio. When minimum and maximum damping levels within a frequency band are considered in SmEdA calculation, they can form upper and lower limits of the cavity-plate energy ratio where experimentally obtained ratio can comply. This gives a deterministic range of an energy ratio for this particular numerical prediction method.

2 SmEdA method for plate-cavity coupled problems

The SmEdA modal coupling loss factor considers both spectral and spatial coupling of discretized subsystem resonances at a coupling surface. Boundary conditions of each uncoupled subsystem are well defined so that their modal information (resonant frequency and modeshape) is easily extracted with the FEM. In equation 1, β_{pq}^{12} is the modal coupling loss factor between the plate mode p of subsystem 1 and the cavity mode q of subsystem 2, and W_{pq}^{12} is the inter-modal work between plate modeshapes and cavity modeshapes. η_p^1 and η_q^2 are the damping loss factors

$$\beta_{pq}^{12} = \frac{W_{pq}^{12}}{M_p^1 M_q^2} \frac{\eta_p^1 \omega_p^1 (\omega_q^2)^2 + \eta_q^2 \omega_q^2 (\omega_p^1)^2}{\left[\left\{(\omega_p^1)^2 - (\omega_p^2)^2\right\}^2 + (\eta_p^1 \omega_p^1 + \eta_q^2 \omega_q^2)\left(\eta_p^1 \omega_p^1 (\omega_q^2)^2\right) + \eta_q^2 \omega_q^2 (\omega_p^1)^2\right]} \quad (1)$$

of the plate mode p of subsystem 1 and the cavity mode q of subsystem 2 respectively. The influence of these two terms on subsystem energy levels are deduced for cases depending on different materials applied to each subsystem: (a) a bare plate coupled to a cavity, (b) a plate subsystem partially treated with a viscoelastic layer, (c) a cavity subsystem partially treated with a porous material. All cases are shown in figure 1. All three cases are first numerically modeled then evaluated through laboratory experiments. The case (b) implements the equivalent single layer modeling of a damped plate. A porous material in case (c) is modeled as an equivalent fluid. The methodology and numerical implementation for case (b) are detailed in [2] [4] [5] [6]. Here, the equivalent fluid modeling for case (c) will be emphasized.

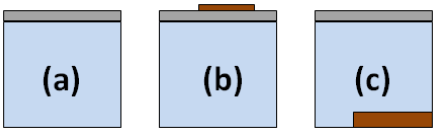

Figure 1. Plate-cavity coupled problems for SmEdA analysis: (a) Bare plate coupled to cavity. (b) Damped plate coupled to cavity. (c) Bare plate coupled to damped cavity

Dimensions of a steel plate and a cavity are 0.5×0.6×0.001 (m) and 0.5×0.6×0.7 (m) respectively. The cavity has five surfaces of the 16 cm thick sold concrete, and its top opening can be covered by a concrete slab of the same thickness. One of the cavity walls has a small hole where microphone cables can be run through. A plate is coupled to a cavity by four metal hinges placed over the plate boundaries and screwed to the top ledges of the cavity.

The dissipative materials are shown in figure 2. The damping pad is a viscoelastic material of a 3 mm thickness. It takes approximately 15 % of the plate surface area. One

and two pads are applied to the plate in case (b). The porous layer is mineral fibres of a 3 cm thickness. Its volume is about 2 % of the cavity.

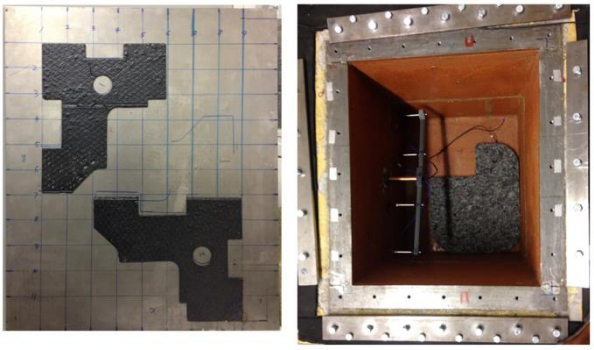

Figure 2. Two damping pads attached to a steel plate (left). A porous material inside a cavity (right)

3 Equivalent fluid modeling of a partially treated cavity

3.1 Porous material modeling

A porous medium is a material containing pores that are typically filled with liquid or gas. The skeleton portion of the material is called a solid frame in which the sound wave can transmit. If the frame is assumed to be not locally reacting e.g. rigid when a porous material is excited by airborne plane waves, it can be modeled as an equivalent fluid characterized by the fluid bulk properties (characteristic impedance, propagation constant, dynamic density and dynamic compressibility) [7] [10]. Such method only corresponds to a treatment on the cavity walls as seen in case (c) of figure 1 e.g. not on or in front of the vibrating plate surface. Equivalent parameters can be deduced from material properties directly measured with an acoustical experiment, which will be given in section 3.2 and 3.3.

The sound propagation inside a porous material is governed by the motion equation and the constitutive law of the medium and is similar to the Helmholtz equation. In equation 2, k_{eq} is a wave number of the equivalent fluid,

$$-K_{eq}\nabla^2 p + \omega^2 \frac{\rho_{eq}}{K_{eq}} = 0 \qquad (2)$$

ρ_{eq} is an equivalent density and K_{eq} is an equivalent compressibility. Then the celerity and the characteristic impedance of the equivalent fluid are complex and frequency dependent:

$$k_{eq} = \omega\sqrt{\rho_{eq}/K_{eq}} \qquad (3)$$
$$Z_c = \sqrt{K_{eq}\cdot\rho_{eq}} \qquad (4)$$
$$c_{eq} = \sqrt{K_{eq}/\rho_{eq}} \qquad (5)$$

In fact, there are several different equivalent fluid models depending on the expressions of parameters. They normally differ by a number of micro scale parameters such as flow resistivity, porosity, tortuosity, characteristic length, etc. that create bulk properties. Empirical models can give equivalent density and fluid wavenumber and are the simplest since they depend on a single parameter, a flow resistivity (σ). Equation 6 and 7 are the Delany-Bazley model and are represented in terms of power law relation:

$$Z_c = \rho c[1 + 0.0571X^{-0.754} - j0.087X^{-0.732}] \qquad (6)$$
$$k_{eq} = \frac{\omega}{c}[1 + 0.0978X^{-0.7} + j0.189X^{-0.595})] \qquad (7)$$

where X = ρf/σ is the adimensional number that quantifies the relative importance of inertial effects [8]. Note that the flow resistivity of the porous material needed for the analytical calculation was given by the manufacture.

3.2 Two-cavity-method

Bulk properties describe the interaction between material and sound wave and are independent of a material thickness and a size. The characteristic impedance and the propagation constant can be derived from a set of distinctive surface impedance measurements (impedance tube measurement) of a porous material. This can be achieved by changing an air depth behind the porous material. This method is called the “two-cavity-method” proposed by Yaniv [9] and Utsuno [10].

As seen in figure 3, a sample layer of the porous material is placed inside the impedance tube for measurements of the "two-cavity-method". Arbitrary acoustic impedances behind the porous sample can be

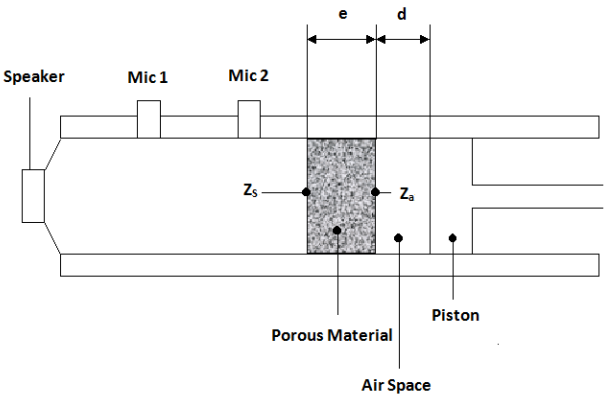

Figure 3. Impedance tube measurement of the "two-cavity-method"

achieved by changing an air space depth behind. The acoustic impedance Z_S at a reference surface can be related to the characteristic impedance Z_c and the propagation constant k_{eq} as follows:

$$Z_c = \pm\sqrt{\frac{Z_{a1}Z_{a2}(Z_{s1}-Z_{s2})-Z_{s1}Z_{s2}(Z_{ai}-Z_{a2})}{(Z_{s1}-Z_{s2})-(Z_{a1}+Z_{a2})}} \qquad (8)$$
$$k_{eq} = \frac{1}{2jd}\ln\left(\frac{Z_{a1}+Z_c}{Z_{a1}-Z_c}\frac{Z_{s1}-Z_c}{Z_{s1}+Z_c}\right) \qquad (9)$$

where Z_{a1} and Z_{a2} are the impedance of a closed tube with different air space depths of L_1 and L_2 respectively, and Z_{s1} and Z_{s2} are the reference surface impedances. The impedances of a closed tube are:

$$Z_{a1} = -j\rho c\ cot(kL_1) \qquad (10)$$
$$Z_{a2} = -j\rho c\ cot(kL_2) \qquad (11)$$

where ρ, c and k are air density, speed of sound and wavenumber respectively.

3.3 Experimental procedure and results

A porous sample with a thickness of 3 cm was cut and placed inside the impedance tube. Following the procedure detailed in [10], Z_c and k_{eq} were obtained from a set of measured surface impedances (Z_{s1} and Z_{s2}) and equation 8 and 9. A big tube with a diameter of 10 cm was used to measure Z_{s1} and Z_{s2} for frequencies up to 1.6 kHz, and a small tube with a diameter of 3 cm was used for a range from 1.6 kHz to 6.4 kHz. Obtained parameters are shown in figure 4. Note that Z_c is normalized with the air impedance (ρc).

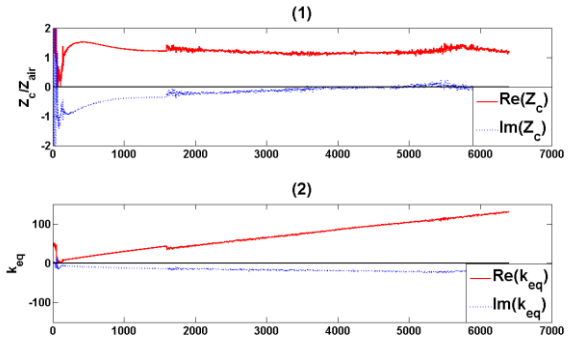

Figure 4. Complex equivalent parameters of the porous material. (1) Normalized characteristic impedance. (2) Fluid wavenumber

Once Z_c and k_{eq} are obtained, the equivalent fluid parameters (c_{eq} and ρ_{eq}) can be deduced with equation (3), (4) and (5). The equivalent celerity and density of the porous material are shown in figure 5. Visible transitions after 1.6 kHz seen in both figure 4 and 5 are due to lesser measurement qualities of the small impedance tube. Nevertheless, the empirical Delany-Bazley model is comparable to experimental results. The real parts of the equivalent celerity and density seen in figure 5 are averaged over 1/3 octave bands then used to calculate resonant frequencies and modeshapes in FEM modeling of an uncoupled damped cavity subsystem of case (c).

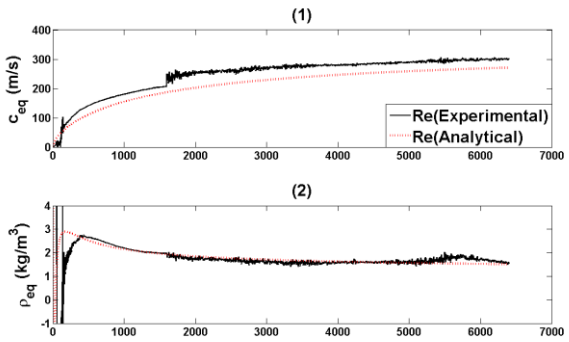

Figure 5. Measured and analytical complex equivalent parameters of the porous material. (1) Real part of equivalent celerity. (2) Real part of equivalent density.

4 Subsystem damping loss factor

In order to give more accurate numerical predictions of subsystem energy levels, experimentally estimated subsystem damping levels (η_1 and η_2) were plugged into equation 1. The damping levels are estimated by the high-resolution modal analysis method detailed in [3]. The subsystem damping for all three cases in figure 1 was considered: 1) a bare plate, 2) an empty cavity, 3) a plate damped with a single damping pad, 4) a plate damped with two damping pads and 5) a damped cavity. Impulse responses were taken at several locations on the plate subsystem and inside the cavity subsystem then damping levels were estimated and averaged from a number of selected resonant peaks for each 1/3 octave band. In figure 6, damping levels of individual modes for a plate damped with a single damping pad are shown in dots, and an average value is shown in line. Figure 7 shows averaged levels of all five subsystems. The influence of the dissipative materials is apparent. However, two damping pads do not double the loss factors compared to those of a single pad. The levels are approximately twice at low frequencies, and the effect diminishes as frequency increases.

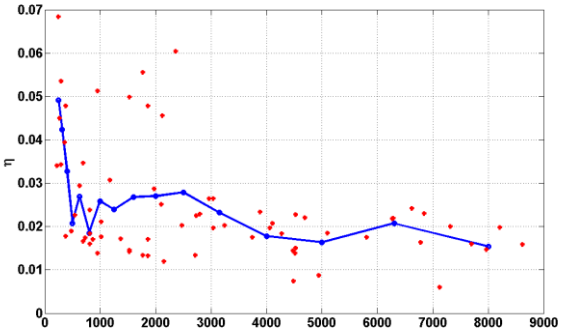

Figure 6. Damping loss factors of the plate treated with a single damping pad (case (b)). The red dot are damping levels of individual modes, and the blue line is an average value in 1/3 octave band.

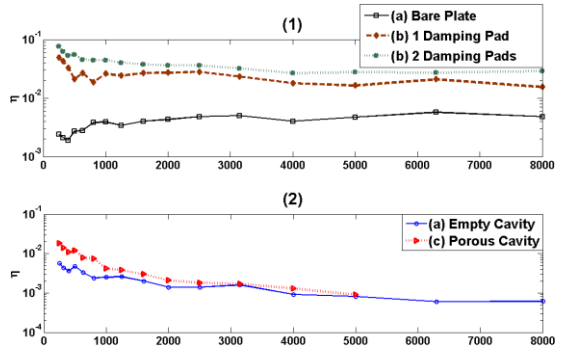

Figure 7. Experimentally estimated subsystem damping loss factors averaged in 1/3 octave band for case (a), (b) and (c). (1) Plate subsystem damping. (2) Cavity subsystem damping.

The damping level (η_1 and η_2) has a direct impact on subsystem energy levels as seen in equation 1. In other words, an accuracy of the SmEdA depends on them. Unless exact damping levels are determined, a numerical

prediction is bound to deviate from an experimental result. Suppose that experimentally obtained damping levels are over or under estimated, then upper and lower bounds of the energy ratio (E_{cavity}/E_{plate}) can be set by considering the lowest and the highest damping levels in frequency bands. Even if an energy ratio deduced from the average damping levels differs from an experimental result, at least its possible deviation range can be predicted for an engineering purpose. Such results will be given in section 5.

5 Subsystem energy relation

5.1 Numerical and experimental procedure

SmEdA subsystem energy levels were deduced as the power was injected into a random position on the plate surface. This was done by solving the SmEdA power flow equation [1]. This was also experimentally done as seen in figure 8. As the plate was excited by a stationary harmonic point force (sweep signal), the plate velocity and the cavity pressure were simultaneously measured and averaged over multiple locations in order to give the subsystem energy levels [11]. A frequency range for case (a) and (b) is up to 10 kHz. Note that a frequency range for case (c) is up to the 5 kHz band since the porous material properties measured with the impedance tube are valid until 6.4 kHz.

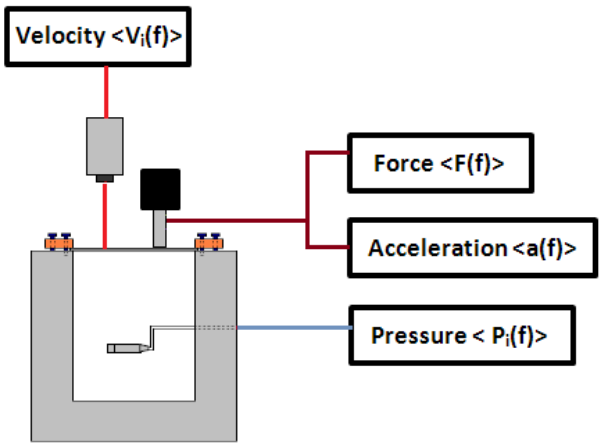

Figure 8. Experimental setup of the plate-cavity coupled structure. Subsystem frequency responses (plate velocity and cavity pressure) are simultaneously measured as the plate is excited. Force and acceleration at the drive point are also measured with an impedance head.

5.2 Result and discussion

Numerically obtained subsystem energy levels for three cases are shown in figure 9. Note that the SmEdA calculations were rendered with average subsystem damping levels. For case (a) and (b), the influence of the damping pad is apparent as seen in figure 9-(1). A single damping pad diminishes the plate energy levels by an average 7.5 dB compared to (a) at all frequencies. Two damping pads do not give twice the damping loss factor as seen in figure 7-(1). However, its effect is almost doubled in plate subsystem energies as the levels are decreased by an average 4 dB more than a single pad. The cavity energy levels also decrease when dissipative materials are applied to either subsystem. However, changes in acoustic energies are smaller between case (b) and (c) than those in plate energies. The effect of the porous material is also clearly seen in figure 9-(2). The porous material reduces the cavity energies by an average 3.5 dB compared to the empty cavity of case (a). Interestingly, the cavity energy levels are reduced more by treating the plate subsystem than directly treating the cavity at almost all frequencies.

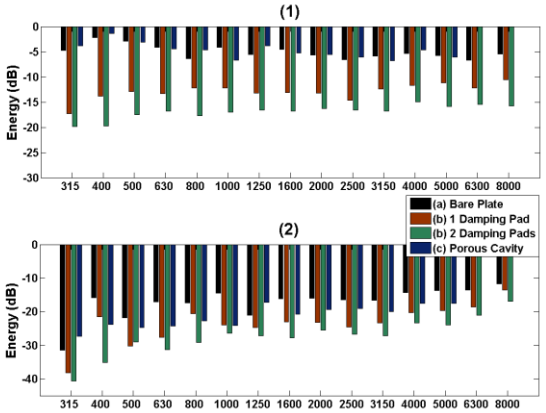

Figure 9. Numerically obtained subsystem energy levels in 1/3 octave bands for case (a), (b) and (c). (1) Plate subsystem energy. (2) Cavity subsystem energy

Subsystem energy levels experimentally obtained are presented in figure 10. The plate energies in figure 10-(1) are in accordance with the numerical results for all cases although the numerical levels are generally overestimated. The differences between plate energies for case (a) and (b) in experimental result are rather small compared to those in numerical result. The same tendencies are shown in the cavity energies as well in figure 10-(2). The SmEdA method can well predict the influence of different damping mechanisms of all three cases but overestimates overall levels.

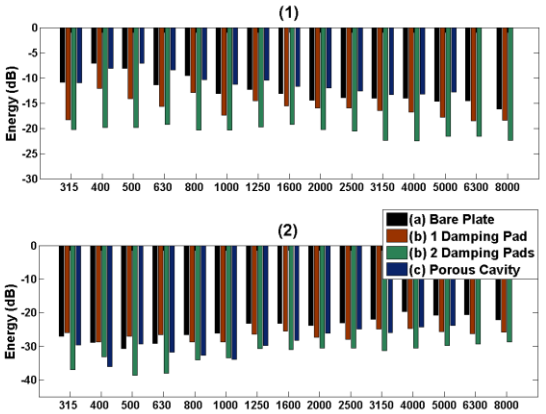

Figure 10. Experimentally obtained subsystem energy levels in 1/3 octave bands for case (a), (b) and (c). (1) Plate subsystem energy. (2) Cavity subsystem energy

Figure 11 shows experimentally obtained subsystem energy ratio (E_{cavity}/E_{plate}) for case (b) in red solid line, when the plate is treated with two damping pads. The upper numerical limit in black dotted line is given when the

lowest damping levels for both subsystems are considered. The highest damping levels then set the lower limit. Experimental result is within the limits only at high frequencies above 1 kHz. The discrepancies at low frequencies could be due to the coupling mechanism in experimental setup. If the plate boundaries are not ideally

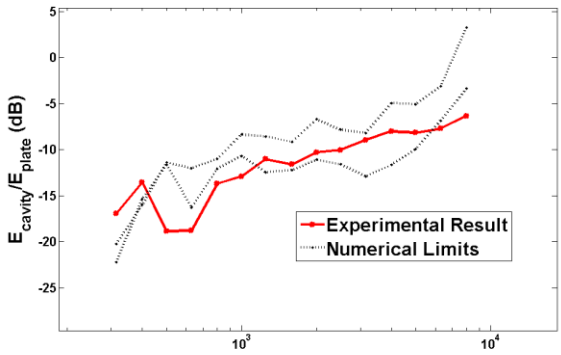

Figure 11. Subsystem energy ratio (E_{cavity}/E_{plate}) in 1/3 octave bands for case (b) when two damping pads are applied.

clamped, this changes the actual dimension of the plate different from that of the finite element model of an uncoupled plate. Such differences can change a number of plate resonant modes and modal orders which can eventually lead to different spectral and spatial couplings with the cavity modes. Then the amount of energy exchanged through these couplings can deviate from numerical predictions.

Figure 12 shows both numerical and experimental energy ratios for all three cases. The dissipative treatment applied to the plate subsystem alone did not result in substantial change compared to case (a). As seen in figure 12-(1) and 12-(2), both numerical and experimental results of case (b) are comparable for the mid-high domain (above 800 Hz). Since the structural treatment resulted in reduction of both subsystem energy levels as seen in figure 9 and 10, their ratios remain almost unchanged. However, the ratio of case (c) is lower than the rest since only the cavity energies are reduced by the porous material. The ratio of case (c) is approximately 4 dB lower than the rest for both numerical and experimental results. This clearly demonstrates a necessity of the direct acoustic response reduction by an absorbing material if a change in subsystem energy ratio is expected.

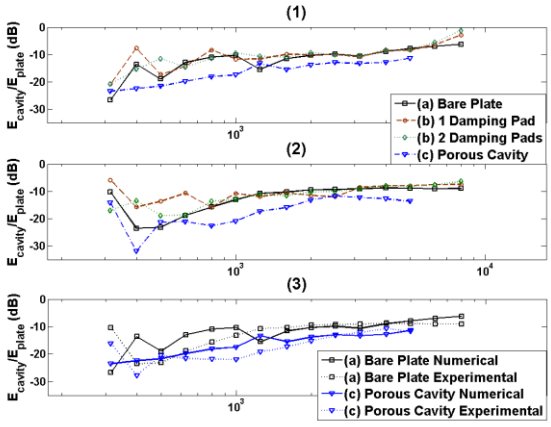

Figure 12. Subsystem energy ratio (E_{cavity}/E_{plate}) in 1/3 octave bands for case (a), (b) and (c). (1) SmEdA predictions. (2) Experimental results. (3) Comparisons between SmEdA prediction and experimental results for case (a) and (c).

Figure 12-(3) shows direct comparisons between numerical and experimental results for case (a) and (c). The numerical predictions are overall comparable to experimental results notably for the mid-high domain. Above 1 kHz, discrepancies between numerical and experimental results are an average 1.7 dB for case (a) and an average 2.2 dB for case (c).

The SmEdA predictions demonstrate overall comparable performance with experimental results for plate-cavity coupled problems. The method can also successfully predict the subsystem energy relation when subsystems are treated with dissipative materials. However, the discrepancies at low frequencies are persistent for all three cases. This could be due to non-ideal boundary condition brought by the coupling mechanism in experimental setup.

6 Conclusion

A plate-cavity coupled problem is investigated in the framework of SmEdA. When each subsystem is treated with dissipative materials (viscoelastic and porous), they can be modeled as equivalent single layer and equivalent fluid respectively. The equivalent properties of a porous material can be deduced from the simple impedance tube measurement of "two-cavity-method." Obtained parameters are complex and frequency dependent.

It is demonstrated that the dissipative treatments have clear influence over subsystem damping levels as well as subsystem energy levels. However, accurate subsystem damping levels are required for deducing correct energy levels. Otherwise, the energy ratio can be predicted within a range whose upper and lower limits can be set by considering the lowest and the highest damping levels in frequency bands. It is also shown that an energy ratio of the cavity subsystem over the plate subsystem is not significantly modified if only the structural subsystem is treated. This can be achieved by treating the cavity subsystem alone with a porous material.

Acknowledgements

This work was co-funded by the French government (FUI 12 - Fonds Unique Interministériel) and European Union (FEDER - Fonds européen de développement régional). It was carried out in the framework of the LabEx CeLyA ("Centre Lyonnais d'Acoustique", ANR-10-LABX-60) and the research project CLIC (“City Lightweight Innovative Cab”) labelled by LUTB cluster (Lyon Urban Truck and Bus), in partnership with Renault Trucks, Arcelor-Mittal, ACOEM, CITI Technologies, FEMTO-ST (Univ. de Franche-Comté) and LVA (INSA de Lyon).

Références

[1] Maxit, L., Guyader, J.-L. Estimation of SEA coupling loss factors using a dual formulation amd FEM modal information, part I: Theory, *Journal of Sound and Vibration*, **293** (5), 907-930, (2001).

[2] Hwang, H. et al. A methodology for including the effect of a damping treatment in the mid-frequency domain using SmEdA method, *Proceedings of the 20th International Congress on Sound and Vibration*, Bangkok, Thailand, 7–11 July, (2013).

[3] Ege, K., Boutillon, X. and David, B. High-resolution modal analysis, *Journal of Sound and Vibration*, **325** (4-5), 852-869, (2009).

[4] Koruk, H., Sanliturk K.Y. Assesment of the complex eigenvalue and the modal strain energy methods for damping predictions, *Proceedings of the 18th International Congress on Sound and Vibration*, Rio de Janeiro, Brazil, 10–14 July, (2011).

[5] Guyader, J.-L., Lesueur, C. Acoustic transmission through orthotropic multilayered plates, part I: Plate vibration modes, *Journal of Sound and Vibration*, **58** (1), 51-68, (1978).

[6] Guyader, J.-L., Cacciolati, C. Viscoelastic properties of singly layer plate material equivalent to multi-layer composites plate, *Proceedings of Inter-Noise*, Istanbul, Turkey, 28-31 August, (2007).

[7] Bécot, F-X., Sgard, F. On the use of poroelastic materials for the control of the sound radiated by a cavity backed plate, *Journal of Acoustical Society of America*, **120** (4), July, (2006).

[8] Dazel, O. et al. Acoustics of porous materials, *Master 2 Acoustique et Mecanique de l'Universite du Maine*, France, (2010).

[9] Utsuno, H et al. Transfer function method for measuring characteristic impedance and propagation constant of porous materials, *Journal of Acoustical Society of America*, **86** (2), August, (1989).

[10] Yaniv, S. Impedance tube measurement of propagation constant and characteristic impedance of porous material, *Journal of Acoustical Society of America*, **54** (5), (1973).

[11] Langhe, K., Sas, P. Statistical analysis of the power injection method, *Journal of Acoustical Society of America*, **100** (1), July, (1996).